

Evanescent coupling between a Raman-active molecule and surface plasmons in ensembles of metallic nanoparticles

T. J. Davis, D. E. Gómez, K. C. Vernon

CSIRO Materials Science and Engineering,

Private Bag 33, Clayton, Victoria, 3168, Australia

Abstract

A theory of surface-enhanced Raman scattering (SERS) is developed based on the coupling between an ensemble of nanoparticles supporting localized surface plasmon resonances (LSPR) and a Raman-active molecule. The molecule is modelled by a dielectric particle supporting many different modes that represent its response to an applied electric field. It is shown how the modes can be modified to include the effects of the vibrational resonances of the molecule that result in Raman scattering and the associated Stokes and anti-Stokes frequency shifts. The same theory can describe the LSPR in an ensemble of metallic nanoparticles of arbitrary shape which leads to a description of the coupling of the evanescent electric fields between the Raman-active molecule and the surface plasmons. The theory predicts the magnitudes of the SERS observed experimentally and can model many of the known Raman effects associated with the LSPR resonances in nanoparticles, including the dependence of the enhancement on the shape and geometry of the nanoparticles, and the effects of the polarization of the incident light. The theory is used to derive an analytical expression for the enhancement associated with a nanoparticle ensemble that exhibits two degenerate modes and it predicts an interference effect arising from the coupling between the modes and the Raman scattering from the molecule.

PACS numbers: xx,xx

I. INTRODUCTION

Since the first experiments demonstrating that surface-enhanced Raman scattering (SERS) from single metal nanoparticles and nanoparticle clusters could be large enough to detect single molecules^{1,2}, there has been a renewed interest in understanding this enhancement. In particular, the development of methods for fabricating metal structures, whether using chemical synthesis or lithography, has led researchers to further investigate the SERS effect to facilitate the design of Raman-enhancing metallic nanoparticle systems. It has been generally agreed that the main contribution to the enhancement arises from the large electric fields associated with surface plasmons in the metal particles, an effect that has been reviewed extensively³⁻⁸.

Investigations of SERS associated with metal nanoparticles have been carried out experimentally and theoretically. There have been many experimental studies to measure enhancements from different configurations of nanoparticles including dimers⁹ and metal nanorods¹⁰⁻¹⁶. A variety of analytical and numerical techniques have been used to model the electromagnetic enhancements. The analytical methods are mainly based on the Mie solutions to the scattering problem for spherical particles and ellipsoids¹⁷, and numerical methods have been used such as the discrete dipole approximation¹⁸, finite difference methods using adaptive meshes¹⁹, the boundary element method^{9,20}, the T-matrix method applied to spheroids²¹, methods based on the discrete dipole approximation and photonic crystals²², on the finite-difference time-domain²³ and on multipole expansions²⁴.

The surface enhancement effect in metallic nanoparticle systems depends on the electromagnetic coupling between the nanoparticles and on their geometry. The effects of coupling have been studied particularly in relation to nanoparticle dimers where the electric field is enhanced in the region between the nanoparticles^{9,15}, as well in the region between a nanoparticle and the substrate²⁵, which can be interpreted as the nanoparticle interacting with its image charge²⁶.

Of similar importance is the nanoparticle geometry. The effect of geometry was observed in the work of Nie and Emory¹ who saw large enhancements both with clusters of spherical nanoparticles and on a nanoparticle rod. The modeling of the coupling effects with nanoparticles of arbitrary geometry is difficult because of the requirement to find analytical solutions to Maxwell's equations. However, an approximate analytical method was

developed recently for understanding the effects of the coupling of the evanescent electric fields arising from localized surface plasmon resonances (LSPR) in ensembles of metallic nanoparticles²⁷⁻³⁰. This method was based on the electrostatic approximation that neglects the effects of retardation³¹⁻³³. Nevertheless, by representing the LSPR as surface charge and surface dipole eigenfunctions it is possible to develop an analytical theory that can accommodate nanoparticles of virtually any shape. The method is capable of predicting many of the observed effects of coupling, such as Fano resonances, the plasmonic equivalent of electromagnetic induced transparency (PEIT) and subradiant modes (dark modes)^{27,30}.

In this paper we apply the evanescent coupling theory^{27,30} to the problem of the Raman enhancement associated with a small number of coupled nanoparticles. In section II we briefly review the theory of coupling of evanescent electric fields valid for nanoparticles much smaller than the wavelength of light. The effect of a molecule that introduces a Raman frequency shift in the field is included in the theory through the polarizability. The result is a general expression describing the excitation of an ensemble of metallic nanoparticles that support localized surface plasmon (LSP) resonances in the presence of a Raman-active molecule. The theory is used to study the interaction between a single nanoparticle and a molecule in section III. A formula for the Raman enhancement factor is derived that is applicable to nanoparticles of any shape. It is shown that the resonant mode of the nanoparticle, which is strongly affected by the shape, plays a dominant role in the enhancement. The theory is used to calculate the enhancements for gold spheres and rods. The effect of multiple particles is discussed in section IV. By representing an ensemble of nanoparticles as a single complex particle with two dominant resonant modes, it is shown how a Raman-active molecule can couple to both modes. An example is given of an ensemble of four coupled nanoparticles with two degenerate modes that demonstrate destructive and constructive interference between the Raman-shifted light fields.

II. NANOPARTICLE COUPLING AND RAMAN-ACTIVE MOLECULES

In this section we adapt the formalism of the electrostatic coupling theory^{27,30} to describe the frequency shifts associated with Raman-active molecules in the presence of an ensemble of metallic nanoparticles. The LSP resonances in the metallic nanoparticles are described using an "electrostatic" eigenmode method^{31,32}. The method is applicable to nanoparticles

much smaller than the wavelength of light and provides useful analytical formulas that can describe the LSPR in particles of any shape. It has been used in numerical simulations to model the electromagnetic Raman enhancements associated with non-spherical nanoparticles interacting with single molecules²⁰. The method involves a set of eigenfunctions that each represent a particular resonant mode. The LSP mode can be excited by an externally applied light field and we represent the strength of this excitation by an amplitude. When isolated, the excitation amplitude $a_n^k(\omega)$ of mode k of nanoparticle n has the form³³

$$\begin{aligned} a_n^k(\omega) &= f_n^k(\omega) \oint \tau_n^k(\vec{r}) \hat{n}_n \cdot \vec{E}_0(\omega) dS \\ &= f_n^k(\omega) \vec{p}_n^k \cdot \vec{E}_0(\omega), \end{aligned} \quad (1)$$

where the integral is over the surface of the nanoparticle, $\tau_n^k(\vec{r})$ is the surface-dipole eigenfunction, \hat{n}_n the surface normal at \vec{r} and $\vec{E}_0(\omega)$ is the incident electric field. Since this field is approximately constant over the nanoparticle surface, it can be taken outside of the integral, which is then equal to a vector $\vec{p}_n^k = \oint \tau_n^k(\vec{r}) \hat{n}_n dS$ that is proportional to the dipole moment of the mode. The resonance factor $f_n^k(\omega)$ contains the information that determines the resonant frequency

$$f_n^k(\omega) = \frac{2\gamma_n^k \epsilon_b (\epsilon(\omega) - \epsilon_b)}{\epsilon_b (\gamma_n^k + 1) + \epsilon(\omega) (\gamma_n^k - 1)}, \quad (2)$$

where γ_n^k is the eigenvalue that depends on the shape of the nanoparticle, $\epsilon(\omega)$ is the electric permittivity of the nanoparticle and ϵ_b is the electric permittivity of the background medium. It can be shown that in the vicinity of the nanoparticle resonance, the resonance factor can be represented by a Lorentzian³⁰. We will use this fact in section III below. The resonance factor is closely related to the polarizability α which plays a fundamental role in the Raman enhancement process. For example, the eigenvalue for the fundamental mode of a sphere is $\gamma_s^1 = 3$ which leads to a resonance factor of

$$\begin{aligned} f_s^1(\omega) &= \frac{3\epsilon_b (\epsilon(\omega) - \epsilon_b)}{2\epsilon_b + \epsilon(\omega)} \\ &= \epsilon_b \alpha / V_s, \end{aligned} \quad (3)$$

where $V_s = 4\pi R_s^3/3$ is the volume of the sphere. In this regard, the resonance factor (2) can be thought of as a polarizability density. The shape of the particle determines the spatial distribution of the surface-charge and the surface-dipole modes, which are represented by the functions $\sigma_n^k(\vec{r})$ and $\tau_n^k(\vec{r})$ and the shape determines the eigenvalue γ_n^k which is a controlling term in the resonance factor $f_n^k(\omega)$.

If the surface-charge $\sigma_n^k(\vec{r})$ and the surface-dipole $\tau_n^k(\vec{r})$ eigenfunctions are suitably normalized, then the dipole moment \vec{p}_n^k associated with mode n can be calculated using either eigenfunction²⁸. In particular, the dipole moment is proportional to the first moment of the surface-charge eigenfunction $\sigma_n^k(\vec{r})$, so that the dipole moment of a nanoparticle with many resonant modes is given by a sum over the excitation amplitudes according to

$$\begin{aligned}\vec{p}_n(\omega) &= \sum_k a_n^k(\omega) \oint \sigma_n^k(\vec{r}) \vec{r} dS \\ &= \sum_k a_n^k(\omega) \vec{p}_n^k.\end{aligned}\tag{4}$$

Combining (1) and (4) leads to

$$\begin{aligned}\vec{p}_n(\omega) &= \sum_k f_n^k(\omega) \vec{p}_n^k (\vec{p}_n^k \cdot \vec{E}_0(\omega)) \\ &= \epsilon_b \sum_k \bar{\alpha}_n^k(\omega) \cdot \vec{E}_0(\omega),\end{aligned}\tag{5}$$

which is written in terms of a frequency-dependent polarizability tensor $\bar{\alpha}_n^k(\omega) = f_n^k(\omega) \vec{p}_n^k \vec{p}_n^k / \epsilon_b$ for each mode of the nanoparticle. The time dependence of the dipole moment is obtained by applying a Fourier transform³³ with the result

$$\vec{p}_n(t) = \epsilon_b \sum_k \int \bar{\alpha}_n^k(t - t') \cdot \vec{E}_0(t') dt'.\tag{6}$$

Our interest is to include in this formalism the frequency shifts that occur with Raman scattering. We will do this by considering the time-dependence of the fields and the excitations of the modes. For a Raman-active molecule, the polarizability can be written in the form³⁴

$$\alpha(t) = \alpha_0 + \alpha_1 e^{-i\nu t},\tag{7}$$

where ν is the frequency of a particular molecular vibration, α_0 is the polarizability for elastic scattering and α_1 determines the effect of the vibrational mode on the polarizability. If we include a large number of vibrations, we can write the time dependence of the polarizability as a sum over the vibrational modes

$$\alpha(t) = \sum_{\nu} \alpha_{\nu} e^{-i\nu t},\tag{8}$$

so that the induced dipole moment $\vec{p}(t)$ in the presence of the time dependent applied field $\vec{E}_0 \exp(-i\omega_0 t)$ is

$$\vec{p}(t) = \epsilon_b \alpha(t) \vec{E}_0 e^{-i\omega_0 t}.\tag{9}$$

Comparing (6) with (9) suggests that we should multiply the polarizability tensor by an additional time-dependent factor that contains the vibrational resonances of the particle. We introduce a Raman scale factor R_n^ν into the expression for the excitation amplitude of nanoparticle n

$$a_n^k(t) = \sum_{\nu} R_n^\nu e^{-i\nu t} \int f_n^k(t-t') \vec{p}_n^k \cdot \vec{E}_0(t') dt'. \quad (10)$$

The Raman scale factor depends on the frequency of the molecular vibrations and has a value such that it corrects the resonance factor f_n^k to give the correct amplitude for the Raman scattering. However, the details of this factor are unimportant because, as we show below, the Raman surface enhancement factor M for individual Raman modes is independent of R_n^ν . The inverse Fourier transform of (10) leads to the equivalent of (1) that includes the effect of Raman scattering

$$a_n^k(\omega + \nu) = \sum_{\nu'} R_n^{\nu-\nu'} f_n^k(\omega + \nu') \vec{p}_n^k \cdot \vec{E}_0(\omega + \nu'). \quad (11)$$

In this paper, we consider the incident field to have a well-defined frequency so that we take the frequency dependence as implicit. Furthermore, we will write the dependence on the Raman frequency ν as an index, which simplifies the expression

$$a_n^{k,\nu} = \sum_{\nu'} R_n^{\nu-\nu'} f_n^{k,\nu'} \vec{p}_n^k \cdot \vec{E}_0^{\nu'} \delta^{0\nu'}. \quad (12)$$

The delta function picks out the term in the sum that depends on the non-Raman shifted incident electric field. Note that the Raman scale factor acts like a frequency shift operator, converting a field at frequency ν' to one at ν .

We now consider an ensemble of interacting nanoparticles with excitation amplitudes $\tilde{a}_n^{k,\nu}$ that depend on the applied field and on the electric fields $\vec{E}_m^\nu(\vec{r})$ arising from all the other nanoparticles m . These fields depend on the Raman frequency as they may arise from Raman-active particles. Then the excitation amplitude in the system of interacting nanoparticles is given by

$$\tilde{a}_n^{k,\nu} = \sum_{\nu'} R_n^{\nu-\nu'} f_n^{k,\nu'} \oint \tau_n^k(\vec{r}) \hat{n}_n \cdot (\vec{E}_0 + \sum_m \vec{E}_m^{\nu'}(\vec{r})) dS, \quad (13)$$

where we have kept the electric fields inside the surface integral since some of these are evanescent fields arising from neighboring nanoparticles with a strong spatial dependence.

The electric field from nanoparticle m arises from the surface-charges according to Coulomb's law

$$\vec{E}_m^\nu(\vec{r}) = \sum_j \tilde{a}_m^{j,\nu} \frac{1}{4\pi\epsilon_b} \oint \sigma_m^j(\vec{r}_m) \frac{(\vec{r} - \vec{r}_m)}{|\vec{r} - \vec{r}_m|^3} dS. \quad (14)$$

Combining (12), (13) and (14) yields

$$\tilde{a}_n^{k,\nu} = a_n^{k,\nu} + \sum_{m,j,\nu'} R_n^{\nu-\nu'} f_n^{k,\nu'} G_{nm}^{kj} \tilde{a}_m^{j,\nu'}, \quad (15)$$

where

$$G_{nm}^{kj} = \frac{1}{4\pi\epsilon_b} \oint \oint \frac{\hat{n}_n \cdot (\vec{r}_n - \vec{r}_m)}{|\vec{r}_n - \vec{r}_m|^3} \tau_n^k(\vec{r}_n) \sigma_m^j(\vec{r}_m) dS_m dS_n, \quad (16)$$

is the geometric coupling coefficient. We define $G_{nn}^{kj} = 0$ since we take the particle as not coupled to itself. Re-arranging (15) gives

$$\sum_{m,j,\nu'} \left(\delta_{nm} \delta^{kj} \delta^{\nu\nu'} - R_n^{\nu-\nu'} f_n^{k,\nu'} G_{nm}^{kj} \right) \tilde{a}_m^{j,\nu'} = a_n^{k,\nu}, \quad (17)$$

which is an equation linking the excitation amplitudes for the nanoparticles in a coupled system to their excitation amplitudes when isolated.

The matrix equation (17) can be inverted to express the excitation amplitudes of the coupled nanoparticle systems in terms of the uncoupled excitation amplitudes

$$\tilde{a}_n^{k,\nu} = \sum_{m,j,\nu'} \left(\delta_{nm} \delta^{kj} \delta^{\nu\nu'} - R_n^{\nu-\nu'} f_n^{k,\nu'} G_{nm}^{kj} \right)^{-1} a_m^{j,\nu'}. \quad (18)$$

This equation is applicable to any number of plasmonic nanoparticles of arbitrary shape interacting with Raman-active molecules. It depends on the Coulomb interaction between the LSPR, represented by G_{nm}^{kj} , on the polarizability of the particle, in terms of $f_n^{k,\nu}$, and on the Raman scale factor, $R_n^{\nu-\nu'}$, that represents the effects of the molecular vibrations. As ν is varied, (18) picks out the various Raman peaks, since $a_n^{k,0}$ represents the isolated molecule excited by an incident field $\vec{E}_0 \exp(-i\omega_0 t)$. By including both positive and negative frequencies in the sum over the Raman modes, then we obtain the direct Rayleigh, or elastic, scattering term for $\nu = 0$, the Stokes lines for $\nu > 0$ and the anti-Stokes lines for $\nu < 0$.

In the following sections we first consider a Raman-active molecule coupled to a single nanoparticle exhibiting LSP resonances and derive an expression for the surface enhancement factor. We then consider more complex systems consisting of multiple nanoparticles.

III. A RAMAN ACTIVE MOLECULE COUPLED TO A SINGLE PLASMONIC NANOPARTICLE

Here we give an example of the coupling of a Raman active molecule to a single plasmonic nanoparticle using (18). We first derive an expression for the SERS enhancement. Since the radiation scattered from a particle is proportional to the square of the induced dipole moment, we base the enhancement factor on the ratio of the dipole moments of the coupled system to that of the isolated molecule.

A. SERS enhancement

We model the molecule as a small dielectric sphere with an excitation amplitude $a_m^{1,\nu}$ where ν runs through the vibrational modes. For simplicity we will assume that multiple Raman modes do not couple to one another through the plasmonic nanoparticles. This allows us to treat the molecule as having only one Raman-active vibrational mode ν in (18). Apart from its Raman-activity, the molecule is not at resonance so that its response to an applied light field is dominated by its fundamental dipole mode. In this case we need only consider one resonant mode so that the amplitude associated with Rayleigh scattering from the molecule is written as $a_m^{1,0}$ where the superscript 1 represents the fundamental dipole resonance of the sphere. Strictly, for a dielectric sphere, the dipole mode is triply degenerate corresponding to the dipole oriented in each of the three orthogonal directions in space²⁸. We assume the plasmonic nanoparticle p has a single mode and it is not Raman active, so that its excitation amplitude when isolated is given by $a_p^{1,0}$. This means that $R_p^0 = 1$ and $R_p^\nu = 0$. However, we note that the amplitude of the nanoparticle must contain the frequency dependence ν because it interacts with the Raman-shifted fields from the molecule. Then from (18) we have

$$\begin{bmatrix} \tilde{a}_p^{1,0} \\ \tilde{a}_p^{1,\nu} \\ \tilde{a}_m^{1,0} \\ \tilde{a}_m^{1,\nu} \end{bmatrix} = \begin{bmatrix} 1 & 0 & -f_p^{1,0} G_{pm}^{1,1} & 0 \\ 0 & 1 & 0 & -f_p^{1,\nu} G_{pm}^{1,1} \\ -f_m^{1,0} G_{mp}^{1,1} & -R_m^{-\nu} f_m^{1,\nu} G_{mp}^{1,1} & 1 & 0 \\ -R_m^\nu f_m^{1,0} G_{mp}^{1,1} & -f_m^{1,\nu} G_{mp}^{1,1} & 0 & 1 \end{bmatrix}^{-1} \begin{bmatrix} a_p^{1,0} \\ 0 \\ a_m^{1,0} \\ a_m^{1,\nu} \end{bmatrix}, \quad (19)$$

where $a_p^{1,\nu} = 0$ because the plasmonic particle is not Raman active. To write down the matrix inverse in (19), we let $g_m^\nu = f_m^{1,\nu} G_{mp}^{1,1}$ and $g_p^\nu = f_p^{1,\nu} G_{pm}^{1,1}$. Then the coupling equation becomes

$$\begin{bmatrix} \tilde{a}_p^{1,0} \\ \tilde{a}_p^{1,\nu} \\ \tilde{a}_m^{1,0} \\ \tilde{a}_m^{1,\nu} \end{bmatrix} = \frac{1}{\Delta_4} \begin{bmatrix} I^\nu & g_p^0 R_m^{-\nu} g_m^\nu & g_p^0 I^\nu & g_p^0 R_m^{-\nu} g_m^\nu g_p^\nu \\ g_p^\nu R_m^\nu g_m^0 & I^0 & g_p^\nu R_m^\nu g_m^0 g_p^0 & g_p^\nu I^0 \\ (I^\nu + R_m^{-\nu} g_m^\nu g_p^\nu R_m^\nu) g_m^0 & R_m^{-\nu} g_m^\nu & I^\nu & R_m^{-\nu} g_m^\nu g_p^\nu \\ R_m^\nu g_m^0 & (I^0 + R_m^\nu g_m^0 g_p^0 R_m^{-\nu}) g_m^\nu & R_m^\nu g_m^0 g_p^0 & I^0 \end{bmatrix} \begin{bmatrix} a_p^{1,0} \\ 0 \\ a_m^{1,0} \\ a_m^{1,\nu} \end{bmatrix}, \quad (20)$$

where we have introduced the following abbreviations $I^0 = 1 - g_p^0 g_m^0$ and $I^\nu = 1 - g_p^\nu g_m^\nu$. The determinant is given by

$$\Delta_4 = (1 - g_m^\nu g_p^\nu)(1 - g_m^0 g_p^0) - R_m^\nu R_m^{-\nu} g_m^0 g_p^0 g_m^\nu g_p^\nu. \quad (21)$$

In surface-enhanced Raman scattering, the molecule is placed near a plasmonic particle that has a significantly larger excitation amplitude. In effect, the plasmonic particle acts as an optical antenna, absorbing the incident light and transferring the energy to the molecule, and then taking the Raman-shifted energy from the molecule and re-radiating it. The amplitude of the Raman-shifted scattering from the plasmonic particle is obtained from the second row of terms in the matrix in (20) which is

$$\tilde{a}_p^{1,\nu} = \frac{1}{\Delta_4} (g_p^\nu R_m^\nu g_m^0 a_p^{1,0} + g_p^\nu R_m^\nu g_m^0 g_p^0 a_m^{1,0} + g_p^\nu I^0 a_m^{1,\nu}). \quad (22)$$

In the situation where the scattering from the molecule is weak compared to that from the nanoparticle, which is usually the case, we have both $a_m^{1,0}$ and $a_m^{1,\nu}$ small and since the resonance factor for the molecule is small then $\Delta_4 \approx 1$, and therefore

$$\tilde{a}_p^{1,\nu} \approx g_p^\nu R_m^\nu g_m^0 a_p^{1,0} = R_m^\nu f_p^{1,\nu} f_m^{1,0} G_{pm}^{1,1} G_{mp}^{1,1} a_p^{1,0}. \quad (23)$$

We can represent the induced dipole moment of the uncoupled nanoparticle using (4) and, similarly, we can represent the dipole moment associated with Raman scattering from the molecule as $\vec{p}_m = R_m^\nu f_m^{1,0} \vec{p}_m^{\vec{1}} (\vec{p}_m^{\vec{1}} \cdot \vec{E}_0)$. If we define the polarization of the incident beam as $\hat{e}_0 = \vec{E}_0 / E_0$ then the ratio of the dipole moments in direction \hat{e} of the Raman-shifted light from the plasmonic nanoparticle to that from the molecule is

$$\frac{\hat{e} \cdot \vec{p}_p}{\hat{e} \cdot \vec{p}_m} = f_p^{1,\nu} f_p^{1,0} G_{pm}^{1,1} G_{mp}^{1,1} \frac{(\hat{e} \cdot \vec{p}_p^{\vec{1}}) (\vec{p}_p^{\vec{1}} \cdot \hat{e}_0)}{(\hat{e} \cdot \vec{p}_m^{\vec{1}}) (\vec{p}_m^{\vec{1}} \cdot \hat{e}_0)}, \quad (24)$$

and the Raman enhancement factor is $M = |\hat{e} \cdot \vec{p}_p / \hat{e} \cdot \vec{p}_m|^2$. This is the key result of this section. It shows that, within the approximations of the derivation, the SERS enhancement does not depend on the Raman scale factor R_n^ν of the molecule, that determines the shape of the Raman spectrum. This is often found in practise where the SERS spectrum is an amplified version of the corresponding Raman spectrum.

The enhancement factor depends strongly on the resonance factors $f_p^{1,\nu} f_p^{1,0}$ at the incident and Raman-shifted frequencies, which corresponds to the polarizabilities of the nanoparticle at these frequencies. The resonance factor for a sphere is given in (3) which can be written in terms of refractive indices m , $f_p^{1,\nu} f_p^{1,0} \propto (m_0^2 - 1)(m_\nu^2 - 1)/(m_0^2 + 2)(m_\nu^2 + 2)$ where $\epsilon_b = 1$, $\epsilon(\omega) = m_0^2$ and $\epsilon(\omega + \nu) = m_\nu^2$. This result was obtained by Kerker et al.¹⁷ who modelled the SERS effects based on a Mie solution for a dielectric sphere. The frequency dependence of the resonance factors is important as it can lead to a distortion of the Raman spectrum. Close to resonance ω_R , these two terms depend on frequency according to

$$f_p^{1,\nu}(\omega) f_p^{1,0}(\omega) \sim \frac{1}{(\delta\omega + \nu + i\Gamma/2)(\delta\omega + i\Gamma/2)}, \quad (25)$$

where $\delta\omega = \omega - \omega_R$ is the deviation from resonance³⁰ and Γ is the dielectric loss term. This equation shows an asymmetry such that features in the Raman spectrum at frequencies beyond the resonance of the nanoparticle have a reduced enhancement compared to features close to resonance. That is, high frequency molecular vibrations are not enhanced as strongly as low frequency vibrations when the incident light is tuned to the resonance of the nanoparticle. This effect has been observed experimentally using lithographically fabricated pairs of nanorods¹⁴.

The enhancement also depends on the the polarization of the light relative to the LSP dipole moment, as has been demonstrated experimentally¹². Also of importance is the dependence of the enhancement on the eigenvalue of the nanoparticle resonance, which is contained in the resonance factor (2). This factor is strongly shape dependent and we will show in the next section that the enhancement varies with the eighth power of the resonance factor. The enhancement also depends on the geometric coupling between the nanoparticle and the molecule such that strong coupling is favoured and the nanoparticle should be at resonance so that the resonance factor is large. These results are well-known. However, our model is not restricted to a single nanoparticle but can include an ensemble of nanoparticles, as in (18).

B. Estimate of the enhancement factor

An estimate of the magnitude of the enhancement can be obtained as follows. The dipole moments of the modes of the molecule can be obtained from a model of the molecule as a small dielectric sphere²⁸, which leads to the form $(\hat{e} \cdot \vec{p}_m^1)(\vec{p}_m^1 \cdot \hat{e}) = (4\pi/3)R_m^3$ where R_m is the effective radius of the molecule. The term for the plasmonic particle can be written in a similar form $(\hat{e} \cdot \vec{p}_p^1)(\vec{p}_p^1 \cdot \hat{e}) = (4\pi/3)R_p^3$ where R_p is the radius of a sphere that has an equivalent volume to the nanoparticle. If the nanoparticle is excited close to resonance, the excitation amplitude can be written in the approximate form³⁰

$$f_p^{1,\nu}(\omega) \approx \frac{-2\gamma_p^{12}\epsilon_b^2\omega_R^3}{(\gamma_p^1 - 1)^2\omega_P^2(\omega + \nu - \omega_R + i\Gamma/2)}, \quad (26)$$

where ω_R is the resonance frequency, γ_p^1 is the eigenvalue for the resonance and ϵ_b is the permittivity of the background medium³⁰. Here we have assumed a Drude model for the permittivity of the metal where ω_P is the plasma frequency and Γ is the loss term. For ν small so that $f_p^{1,\nu} \approx f_p^{1,0}$, then placing (26) into (24) gives

$$\frac{\hat{e} \cdot \vec{p}_p}{\hat{e} \cdot \vec{p}_m} = \left(\frac{\gamma_p^1}{\gamma_p^1 - 1} \right)^4 \left(\frac{4\epsilon_b^4 G_{mp}^{1,1} G_{pm}^{1,1}}{(\omega - \omega_R + i\Gamma/2)^2} \right) \left(\frac{\omega_R^3}{\omega_P^2} \right)^2 \left(\frac{R_p^3}{R_m^3} \right). \quad (27)$$

At resonance we have $\omega = \omega_R$ and the enhancement depends on the geometric coupling and on the loss term associated with the metal. For both gold and silver in the visible spectrum near 700 nm³⁵, we find that $\Gamma\omega_P^2/\omega_R^3 \sim 1$. For a molecule coupling to a plasmonic nanoparticle, the coupling terms have been estimated²⁸ as $4\epsilon_b^4 G_{mp}^{1,1} G_{pm}^{1,1} \approx (\kappa\epsilon_b^2/3\pi)(R_m/R_{mp})^3$ where R_m is the effective radius of the molecule, R_{mp} is the area on the plasmonic particle over which the molecule interacts and κ is a constant of the order of 1/10 relating to the fraction of the eigenfunctions within the interaction region. With these terms in (27) we have at resonance

$$M = \left| \frac{\hat{e} \cdot \vec{p}_p}{\hat{e} \cdot \vec{p}_m} \right|^2 \approx \left(\frac{4\kappa\epsilon_b^2}{3\pi} \right)^2 \left(\frac{\gamma_p^1}{\gamma_p^1 - 1} \right)^8 \left(\frac{R_p}{R_{mp}} \right)^6. \quad (28)$$

The enhancement factor depends on the eigenvalue γ_p^1 which can be close to 1 for high aspect ratio structures. For example, a sphere has $\gamma_p^1 = 3$ whereas a nanorod with length to diameter ratio of 4 would typically have $\gamma_p^1 \approx 1.15$. Using the nanorod eigenvalue, the 8th power dependence of the factor can lead to an amplitude increase in air of 10⁷. Depending

on the relative size of the nanoparticle and its interaction region with the molecule, the other factors can be several orders of magnitude leading to an additional 10 to 10^4 depending on details.

To maximise the enhancement, we would like to keep the eigenvalue close to 1, which is controlled by the shape of the nanostructure. Furthermore, we would like the nanostructure to be large (R_p large) and the interaction region with the molecule, R_{mp} , to be small. However, we would also require κ to be large since this relates to the fraction of the total charge associated with a LSP mode that interacts with the molecule. This suggests that the optimum coupling region is at a sharp point or a sharp edge of the nanoparticle since the surface charges accumulate there and the interaction region can be small. This approximate formula demonstrates some of the key parameters that determine the SERS enhancements. In the following section we will calculate some of these enhancement factors based on numerical evaluations of the geometric coupling, the resonance factors and the nanoparticle eigenvalues.

C. Enhancement for a sphere

We have calculated the enhancement factors for a sphere and compared them with the literature. The enhancement factor for a gold sphere in water is shown in Fig. 1. The calculations were performed at the sphere resonance, which occurs at 521 nm. They were evaluated using a numerical solution for the eigenmodes of the sphere to determine the geometric coupling terms $G_{mp}^{11}G_{pm}^{11}$ which are then used with the resonance factors, as in (24), to determine the enhancements. In this calculation the Raman-active molecule is modelled by a dielectric sphere with three degenerate dipole modes, corresponding to a dipole oriented in each of the three orthogonal space directions. This is necessary to properly account for the induced dipole in the molecule because the modes excited when the molecule is placed in an electric field combine to give a single dipole oriented in the local direction of the applied field. The enhancements vary with distance and depend on the direction of approach to the surface. The enhancement calculated for the gold sphere is 10^3 . A similar calculation of the enhancement of a silver sphere at resonance in water gives $M = 8 \times 10^5$ which agrees closely with the calculation of Kerker et al.¹⁷ for a silver sphere of 5 nm diameter.

When two spheres are combined, but separated by a small gap (in this example equal

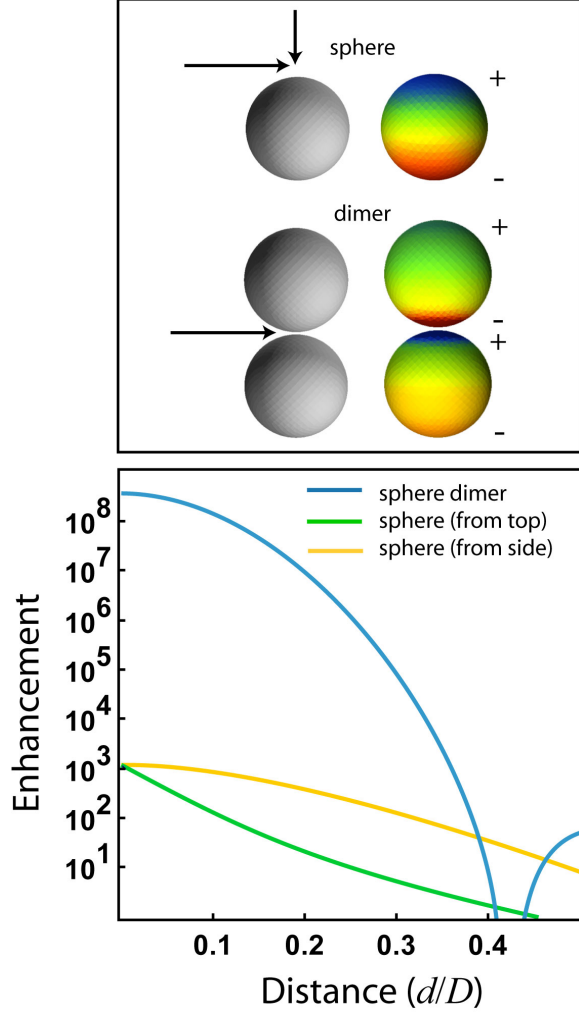


FIG. 1: (Color online) The enhancement factors as functions of distance from the surface of a single sphere and a dimer of spheres, measured in units of the sphere diameter. The enhancements have been calculated for a molecule approaching the surface of the sphere from two directions and the surface of the dimer from one direction, as shown in the figure. The calculations were performed at the resonant wavelengths of the structure, assuming the spheres were made from gold in a background medium of water $\epsilon_b = 1.77$. The resonance was at 521 nm for the single sphere and at 587 nm for the dimer. The colors on the spheres represent the distribution of surface-dipoles associated with the surface plasmon eigenmode.

to $1/50^{th}$ of the sphere diameter) the resonance shifts due to the interaction between the spheres. The coupling of the sphere modes leads to a localization of the surface charge in the vicinity of the gap and an increase in the electric field. The coupling of the spheres with one another and with a Raman-active molecule is given by (18). We have evaluated this

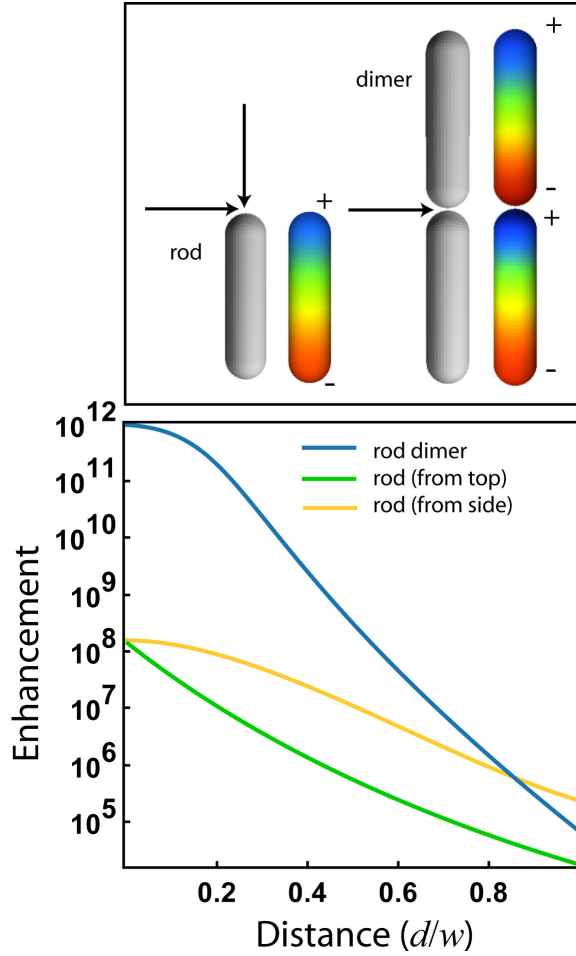


FIG. 2: (Color online) The enhancement factors as functions of distance from the surface of a single rod and a pair of rods, measured in units of the rod diameter. The rod length:width ratio was 3:1 with hemispherical endcaps. The enhancements have been calculated for a molecule approaching the surface from two directions and the surface of the pair of rods from one direction, as shown in the figure. The calculations were performed at the resonant wavelengths of the structure, assuming the rods were made from gold in a background medium of water $\epsilon_b = 1.77$. The resonance was at 809 nm for the single rod and at 934 nm for the pair. The colors on the rods represent the distribution of surface-dipoles associated with the surface plasmon eigenmode.

numerically for a pair of gold spheres in water and find that the resonance shifts to 587 nm. The calculated enhancement has a maximum of 4×10^8 which is consistent with the results of Xu et al.²⁰.

The dimer shows interesting behaviour where the enhancement passes through zero at a particular distance. This is because the dimer has the form of two closely spaced dipoles.

When the molecule is close to the junction between the two spheres, the charges at the junction dominate the enhancement. These charges appear like a dipole with a particular orientation. However, far from the junction the two charges tend to cancel and the molecule is affected more by the distributed surface charges at the ends of each sphere. These act like a dipole oriented oppositely to that at the junction. Therefore, there should be a point where the two effective dipoles cancel one another.

D. Enhancement for a nanorod

We have also calculated the enhancement factors for a gold nanorod as functions of distance, as shown in Fig. 2. The rod is taken to be in water with a permittivity $\epsilon_b = 1.77$. The single rod is resonant at 809 nm. At this wavelength, gold is relatively less absorbing than at 521 nm which is the resonance of the sphere. This partly accounts for the larger enhancement factors. In addition, the rod has an eigenvalue of $\gamma_R = 1.16$ compared to the sphere with $\gamma_S = 3.00$. Since the enhancements depend on γ according to (28) we would expect the rod to have an enhancement ratio about 10^5 times that of a sphere, which comparing the two figures is about the factor we find. The enhancement factors associated with chemically synthesized gold nanorods have been measured experimentally¹¹ yielding $M \approx 10^6$. However, in these experiments the rods had a length:width aspect ratio of 2.7 which corresponds to $\gamma_R = 1.23$ for the fundamental dipole mode and the excitation wavelength was not at the LSP resonance of the rods. Using (28) for the γ dependence, the enhancement factors should be reduced by a factor of 0.08, which is consistent with the experimental observations.

Also shown in Fig. 2 is the enhancement associated with two coupled rods. This shows a significant enhancement over a sphere. Note that the calculations are based on the electrostatic approximation, which has several limitations. Firstly, it is a classical calculation that fails to take account of quantum mechanical effects that are known to create a more diffuse charge cloud and change the boundary conditions, lowering the electric field strength compared to the classical calculation³⁶⁻³⁸. Secondly it does not take account of retardation of the fields, relying on the nanoparticles to be much smaller than the wavelength of light. The effect of retardation was discussed by Wokan et al³⁹ and can be included in the coupling theory as necessary²⁷.

IV. MULTI-PARTICLE COUPLING AND SERS ENHANCEMENT

The interaction of a Raman-active molecule with an ensemble of plasmonic nanoparticles can be analysed by a straightforward application of (18). However, for many particles and many resonant modes the matrix inversion is complicated and yields large expressions. Although it is straightforward to do this numerically, there is value in obtaining analytical relations between the parameters of the system. A way to approach this problem is to consider the system of nanoparticles as a single entity. That is, we can treat the nanoparticle ensemble as some complicated nanostructure with a set of resonant modes. This approach was used by Gómez et al²⁹ to generate a heirarchical set of plasmonic structures where the eigenvalues and eigenfunctions of the coupled system are found in terms of the individual nanoparticles. In this way, we can focus our attention on one or two modes of interest and study how these are coupled to the molecule.

To demonstrate this method, we consider an ensemble of nanoparticles that has two resonant modes near the frequency of interest. The coupling coefficients between the ensemble and the molecule involve an implicit sum over the individual nanoparticles. This sum arises when evaluating (16) where the integral is taken over all of the surfaces in the ensemble. As before we assume that the molecule has only one resonant mode, although in our numerical calculations we will take account of all three degenerate modes. If we make the abbreviations $g_p^{k,\nu} = f_p^{k,\nu} G_{pm}^{k,1}$ and $g_m^{\nu,k} = f_m^{1,\nu} G_{mp}^{1,k}$ then the matrix obtained from (18) is given by

$$\begin{bmatrix} \tilde{a}_p^{1,0} \\ \tilde{a}_p^{1,\nu} \\ \tilde{a}_p^{2,0} \\ \tilde{a}_p^{2,\nu} \\ \tilde{a}_m^{1,0} \\ \tilde{a}_m^{1,\nu} \end{bmatrix} = \begin{bmatrix} 1 & 0 & 0 & 0 & -g_p^{1,0} & 0 \\ 0 & 1 & 0 & 0 & 0 & -g_p^{1,\nu} \\ 0 & 0 & 1 & 0 & -g_p^{2,0} & 0 \\ 0 & 0 & 0 & 1 & 0 & -g_p^{2,\nu} \\ -g_m^{0,1} & -R_m^{-\nu} g_m^{\nu,1} & -g_m^{0,2} & -R_m^{-\nu} g_m^{\nu,2} & 1 & 0 \\ -R_m^{\nu} g_m^{0,1} & -g_m^{\nu,1} & -R_m^{\nu} g_m^{0,2} & -g_m^{\nu,2} & 0 & 1 \end{bmatrix}^{-1} \begin{bmatrix} a_p^{1,0} \\ 0 \\ a_p^{2,0} \\ 0 \\ a_m^{1,0} \\ a_m^{1,\nu} \end{bmatrix}, \quad (29)$$

where we assume that the metallic nanostructures are not Raman active so that $R_p^{\nu} = 0$ and the Raman-shifted amplitudes of the two modes of the isolated structure are zero, $a_p^{1,\nu} = a_p^{2,\nu} = 0$. The matrix in (29) can be inverted and multiplied into the vector on the right. The factors of interest are the excitation amplitudes of the nanostructure at the Raman-shifted frequency. If we assume that the excitation amplitudes of the isolated

molecule are small, so that $a_m^{1,0} \approx 0$ and $a_m^{1,\nu} \approx 0$ then we have

$$\tilde{a}_p^{1,\nu} \approx \frac{R_m^\nu g_p^{1,\nu}}{\Delta_6} (g_m^{0,1} a_p^{1,0} + g_m^{0,2} a_p^{2,0}) \quad (30)$$

$$\tilde{a}_p^{2,\nu} \approx \frac{R_m^\nu g_p^{2,\nu}}{\Delta_6} (g_m^{0,1} a_p^{1,0} + g_m^{0,2} a_p^{2,0}) \quad (31)$$

where the determinant is

$$\begin{aligned} \Delta_6 = & (1 - g_m^{0,1} g_p^{1,0} + g_m^{0,2} g_p^{2,0})(1 - g_m^{\nu,1} g_p^{1,\nu} + g_m^{\nu,2} g_p^{2,\nu}) \\ & - R_m^\nu R_m^{-\nu} (g_m^{0,1} g_p^{1,0} + g_m^{0,2} g_p^{2,0})(g_m^{\nu,1} g_p^{1,\nu} + g_m^{\nu,2} g_p^{2,\nu}). \end{aligned} \quad (32)$$

The determinant controls the shift in the resonance of the nanoparticle due to the presence of the molecule. In most cases the shift is very small because both the molecule resonance factors $f_m^{1,0}$ and $f_m^{1,\nu}$ and the couplings are small, whereupon $\Delta_6 \approx 1$. Converting these equations to enhancement amplitudes, in the same way as in the previous section, leads to the result

$$\begin{aligned} \frac{\hat{e} \cdot \vec{p}_p}{\hat{e} \cdot \vec{p}_m} = & f_p^{1,\nu} f_p^{1,0} G_{pm}^{11} G_{mp}^{11} \frac{(\hat{e} \cdot \vec{p}_p^{\vec{1}})(\vec{p}_p^{\vec{1}} \cdot \hat{e}_0)}{(\hat{e} \cdot \vec{p}_m^{\vec{1}})(\vec{p}_m^{\vec{1}} \cdot \hat{e}_0)} \\ & + f_p^{1,\nu} f_p^{2,0} G_{pm}^{11} G_{mp}^{12} \frac{(\hat{e} \cdot \vec{p}_p^{\vec{1}})(\vec{p}_p^{\vec{2}} \cdot \hat{e}_0)}{(\hat{e} \cdot \vec{p}_m^{\vec{1}})(\vec{p}_m^{\vec{1}} \cdot \hat{e}_0)} \\ & + f_p^{2,\nu} f_p^{1,0} G_{pm}^{21} G_{mp}^{11} \frac{(\hat{e} \cdot \vec{p}_p^{\vec{2}})(\vec{p}_p^{\vec{1}} \cdot \hat{e}_0)}{(\hat{e} \cdot \vec{p}_m^{\vec{1}})(\vec{p}_m^{\vec{1}} \cdot \hat{e}_0)} \\ & + f_p^{2,\nu} f_p^{2,0} G_{pm}^{21} G_{mp}^{12} \frac{(\hat{e} \cdot \vec{p}_p^{\vec{2}})(\vec{p}_p^{\vec{2}} \cdot \hat{e}_0)}{(\hat{e} \cdot \vec{p}_m^{\vec{1}})(\vec{p}_m^{\vec{1}} \cdot \hat{e}_0)} \end{aligned} \quad (33)$$

where we have \vec{p}_p as the total dipole moment associated with the two modes of the nanostructure.

These equations contain the direct Raman coupling term, as in (24), as well as cross-coupling terms which represent the excitation of the molecule by the evanescent fields associated with one mode of the nanostructure and the subsequent excitation of the other mode by the Raman-shifted fields. The structure of this equation is represented diagrammatically in Fig. 3 which shows two modes, their coupling to a molecule, and the subsequent coupling of the Raman-shifted fields back into the two modes. The Raman signal can arise from a number of different paths, such as through an excitation of mode 1, a coupling to the molecule via G_{mp}^{11} , a coupling of the Raman-shifted fields to mode 2 via G_{pm}^{21} and the subsequent radiation. The equation shows a strong dependence on the polarization of the

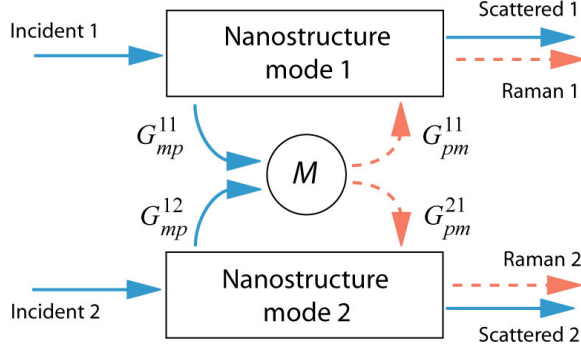


FIG. 3: (Color online) A representation of Eq. (33) that shows the different ways in which light can couple from two modes of a nanostructure into a molecule M and the subsequent out-coupling of the Raman-shifted light through the nanoparticles (shown as dashed lines).

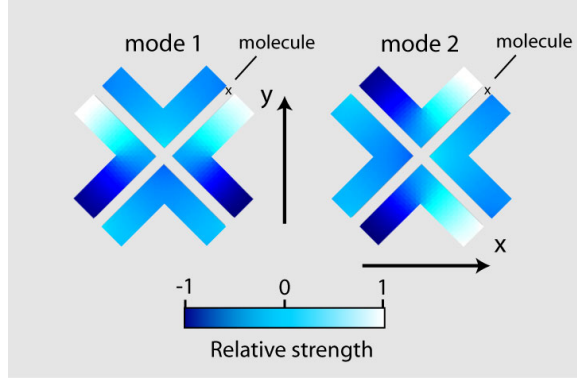


FIG. 4: (Color online) The two degenerate modes of a coupled nanostructure system. The color (grey scale) represents the relative strength of the localized surface plasmon resonances in the structure. The arrows show the directions of the dipole moments associated with each mode. The point where the Raman enhancement is calculated is labelled with 'x'. For nanostructures much smaller than the wavelength of the light, the resonances are independent of the physical dimension³². Each right-angled nanostructure has the relative dimensions 1 unit thick, 4.2 units long and 1.3 units wide and the spacing between them is 0.5 units.

incident field with respect to the orientation of the dipole moments of the LSPR modes, as well as on the polarization of the emitted radiation. Moreover, the cross-coupling of the Raman-shifted fields also depends on the polarization.

A consequence of the cross-coupling is that the Raman signal from one mode can interfere constructively or destructively with the signal from the other mode. We give an example

of this effect using the symmetric four nanoparticle system in Fig. 4. This structure has been contrived so that it has two degenerate modes (as shown) that have dipole moments perpendicular to one another. This allows the excitation of the modes to be controlled by the polarization of the incident beam. Mode 1 of the structure has a dipole moment oriented in the y direction and it will be excited by light polarized in the y direction. Similarly, mode 2 has a dipole moment oriented in the x direction and is excited by x -polarized light. Because the two modes are degenerate and orthogonal, the scattering cross section is independent of the polarization of the incident beam, provided the scattered beam is measured without a polarizer. The molecule placed at the position as marked can be excited by the LSPR for light with either polarization. If there was little or no coupling between the modes we would expect a significant Raman signal independent of the polarization of the incident beam. However, the coupling of the Raman signal between the modes changes this situation. The Raman enhancements associated with the structure are shown in Fig. 5 for incident light with four different polarization directions. The enhancements were calculated using a numerical solution of (18) for a molecule placed at the position as marked in Fig. 4. The enhancements are the same independent of the polarization direction of the radiated light. The polarization angle is taken relative to the x axis. In this calculation the structure is made of gold embedded in a medium of effective permittivity $\epsilon_{\text{eff}} = 1.2$ which mimics the structure on a glass substrate in air, based on the effective medium method²⁶. It is clear that there is destructive interference when the incident beam is polarized at 45° to the x axis and constructive interference at a polarization angle of 135° . The slight asymmetry in the calculated enhancements for 0° and 90° are due to a small geometric distortion in the structure used in the calculation.

In this example the interference arises from the relative phases of the modes and the signs of the surface charges induced in the arms of the nanostructure near the molecule. The destructive interference is associated with surface charges of the same sign on the arms while the constructive interference is due to surface charges with opposite signs.

V. CONCLUSIONS

We have developed a theory of surface-enhanced Raman scattering from molecules based on a theory of the coupling of the evanescent electric fields associated with localized surface

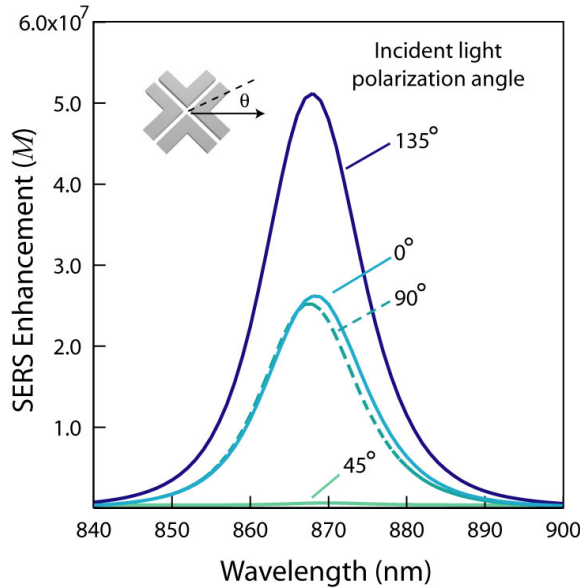


FIG. 5: (Color online) The SERS enhancement M as a function of wavelength for incident light with four different polarizations. This demonstrates the destructive (at 45°) and constructive (at 135°) interference of the enhancement associated with two competing modes. The angle is referenced to the x axis as shown. The nanostructures are assumed to be made from gold on a glass substrate.

plasmons in metallic nanoparticles. Although the theory is approximate, in the sense that it is only applicable to nanostructures smaller than the wavelength of light and it does not take into account retardation, it has been shown to give results consistent with both theory and experiment. For a single particle coupling to a molecule, the theory shows that the nanoparticle acts like an optical antenna, efficiently coupling light energy to the molecule and capturing the Raman-shifted light and re-radiating it. More importantly, the theory describes the Raman scattering, and subsequent enhancements, associated with coupling to an *ensemble* of nanoparticles of arbitrary shape. The geometry dependence is represented by several parameters - the eigenvalue as well as the associated eigenfunctions that, in many cases, can be reduced to dipole moments. An example was given in which the coupling leads to interference between the Raman-scattering between two different modes associated with the ensemble. We anticipate that the theory will be of value in designing nanostructures on a substrate for controlling the surface enhancement, both in terms of intensity, polarization effects and through the resonances of the nanostructures.

Acknowledgments

This work was supported by the Sensors and Sensor Networks Transformational Capability Platform (S&SN TCP) within the Commonwealth Scientific and Industrial Research Organisation, Australia.

- ¹ S. Nie and S. R. Emory, *Science* **275**, 1102 (1997).
- ² K. Kneipp, Y. Wang, H. Kneipp, L. T. Perelman, I. Itzkan, R. R. Dasari, and M. S. Feld, *Physical Review Letters* **78**, 1667 (1997).
- ³ M. Kerker, *Accounts of Chemical Research* **17**, 271 (1984).
- ⁴ H. Metiu and P. Das, *Annual Review of Physical Chemistry* **35**, 507 (1984).
- ⁵ M. Moskovits, *Reviews of Modern Physics* **57**, 783 (1985).
- ⁶ G. A. Baker and D. S. Moore, *Analytical Bioanalytical Chemistry* **382**, 1751 (2005).
- ⁷ M. Moskovits, *Journal of Raman Spectroscopy* **36**, 485 (2005).
- ⁸ P. L. Stiles, J. A. Dieringer, N. C. Shah, and R. P. Van Duyne, *Annual Review of Analytical Chemistry* **1**, 601 (2008).
- ⁹ T. Dadosh, J. Sperling, G. W. Bryant, R. Breslow, T. Shegai, M. Dyshel, G. Haran, and I. Bar-Joseph, *ACS Nano* **3**, 1988 (2009).
- ¹⁰ N. Fellidj, J. Aubard, G. Levi, J. R. Krenn, M. Salerno, G. Schider, B. Lamprecht, A. Leitner, and F. R. Aussenegg, *Physical Review B* **65**, 075419 (2002).
- ¹¹ B. Nikoobakht and M. A. El-Sayed, *The Journal of Physical Chemistry A* **107**, 3372 (2003).
- ¹² J. Grand, M. L. de la Chapelle, J. L. Bijeon, P. M. Adam, A. Vial, and P. Royer, *Physical Review B* **72**, 033407 (2005).
- ¹³ C. J. Orendorff, L. Gearheart, N. R. Jana, and C. J. Murphy, *Physical Chemistry Chemical Physics* **8**, 165 (2006).
- ¹⁴ W. Zhang, H. Fischer, T. Schmid, R. Zenobi, and O. J. F. Martin, *The Journal of Physical Chemistry C* **113**, 14672 (2009).
- ¹⁵ S. Li, M. L. Pedano, S.-H. Chang, C. A. Mirkin, and G. C. Schatz, *Nano Letters* **10**, 17221727 (2010).
- ¹⁶ J. Petschulat, D. Cialla, N. Janunts, C. Rockstuhl, U. Hbner, R. Mller, H. Schneidewind,

- R. Mattheis, J. Popp, A. Tnnermann, et al., *Opt. Express* **18**, 4184 (2010).
- ¹⁷ M. Kerker, D.-S. Wang, and H. Chew, *Appl. Opt.* **19**, 4159 (1980).
- ¹⁸ W.-H. Yang, G. C. Schatz, and R. P. V. Duyne, *Journal of Chemical Physics* **103**, 869 (1995).
- ¹⁹ F. J. Garca-Vidal and J. B. Pendry, *Physical Review Letters* **77**, 1163 (1996).
- ²⁰ H. Xu, J. Aizpurua, M. Kll, and P. Apell, *Physical Review E* **62**, 4318 (2000).
- ²¹ R. Boyack and E. C. L. Ru, *Physical Chemistry Chemical Physics* **11**, 7398 (2009).
- ²² P. Etchegoin, L. F. Cohen, H. Hartigan, R. J. C. Brown, M. J. T. Milton, and J. C. Gallop, *Journal of Chemical Physics* **119**, 5281 (2003).
- ²³ M. Futamata, Y. Maruyama, and M. Ishikawa, *Journal of Molecular Structure* **735**, 75 (2005).
- ²⁴ R. Rojas V and F. Claro, *The Journal of Chemical Physics* **98**, 998 (1993).
- ²⁵ O. J. Glembocki, R. W. Rendell, D. A. Alexson, S. M. Prokes, A. Fu, and M. A. Mastro, *Physical Review B* **80**, 085416 (2009).
- ²⁶ K. C. Vernon, A. M. Funston, C. Novo, D. E. Gómez, P. Mulvaney, and T. J. Davis, *Nano Letters* **10**, 2080 (2010).
- ²⁷ T. J. Davis, K. C. Vernon, and D. E. Gómez, *Physical Review B* **79**, 155423 (2009).
- ²⁸ T. J. Davis, D. E. Gómez, and K. C. Vernon, *Physical Review B* **81**, 045432 (2010).
- ²⁹ D. E. Gómez, K. C. Vernon, and T. J. Davis, *Physical Review B* **81**, 075414 (2010).
- ³⁰ T. J. Davis, D. E. Gómez, and K. C. Vernon, *Nano Letters* **10**, 2618 (2010).
- ³¹ F. Ouyang and M. Isaacson, *Philosophical Magazine B* **60**, 481 (1989).
- ³² I. D. Mayergoyz, D. R. Fredkin, and Z. Zhang, *Physical Review B* **72**, 155412 (2005).
- ³³ I. D. Mayergoyz, Z. Zhang, and G. Miano, *Physical Review Letters* **98**, 147401 (2007).
- ³⁴ N. B. Colthup, L. H. Daly, and S. E. Wiberley, *Introduction to Infrared and Raman Spectroscopy* (Academic Press Inc, New York, 1975), 2nd ed.
- ³⁵ P. Johnson and R. Christy, *Physical Review B* **6**, 4370 (1972).
- ³⁶ V. N. Pustovit and T. V. Shahbazyan, *Physical Review B* **73**, 085408 (2006).
- ³⁷ D. J. Masiello and G. C. Schatz, *Physical Review A* **78**, 042505 (2008).
- ³⁸ J. Zuloaga, E. Prodan, and P. Nordlander, *Nano Letters* **9**, 887 (2009).
- ³⁹ A. Wokaun, J. P. Gordon, and P. F. Liao, *Physical Review Letters* **48**, 957 (1982).